Nanostructured Thin Films of C_{60} – Aniline Dyad Clusters: Electrodeposition, Charge Separation, and Photoelectrochemistry

Prashant V. Kamat,*[a] Said Barazzouk,[a, b] Surat Hotchandani,[b] and K. George Thomas[a, c]

Abstract: Clusters of C_{60} – aniline dyads are deposited as thin films on nanostructured SnO_2 electrodes under the influence of an electric field. At low applied DC voltage (< 5 V) the clusters in toluene/acetonitrile (1:3) mixed solvent grow in size (from 160 nm to $\sim$200 nm in diameter) while at higher voltages (> 50 V) they are deposited on the electrode surface as thin films. The C_{60} – aniline dyad cluster films when cast on nanostructured SnO_2 films are photoelectrochemically active and generate photocurrent under visible light excitation. These nanostructured fullerene films are capable of delivering relatively large photocurrents (upto $\sim$0.2 mA cm^{-2}, photoconversion efficiency of 3 – 4 %) when employed as photoanodes in photoelectrochemical cells. Both luminescence and transient absorption studies confirm the formation of charge transfer product (C_{60} anion) following UV/Vis excitation of these films. Photo-induced charge separation in these dyad clusters is followed by the electron injection from C_{60}-anion moiety into the SnO_2 nanocrystallites. The oxidized counterpart is reduced by the redox couple present in the electrolyte, thus regenerating the dyad clusters. The feasibility of casting high surface area thin fullerene films on electrode surfaces has opened up new avenues to utilize dyad molecules of sensitizer bridge donor type in light energy conversion devices, such as solar cells.

Keywords: donor – acceptor systems · electron transfer · fullerenes · nanostructures · photoelectrochemistry · thin films

Introduction

C_{60} – bridge – donor dyads are an interesting class of compounds that are capable of undergoing charge separation following photoexcitation.[1–5] Several research groups have focussed their efforts towards achieving efficient charge separation and stabilization of the electron-transfer products. Excited-state properties of fullerene-based dyads, particularly the photoinduced electron transfer processes, have been extensively investigated because of their potential applications in photovoltaic and optoelectronic devices.[6–9] A feasible approach to utilize the photo-induced charge separation in fullerene – donor dyad molecule would be to transfer the electrons from the fullerene anion into a semiconductor nanoparticle (Scheme 1) and utilize it for photocurrent generation. The possibility of employing fullerenes and functionalized fullerenes for photoelectrochemical and photovoltaic cells has already been demonstrated.[10–13]

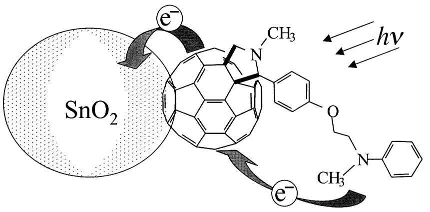

Scheme 1. Propsed electron transfer from the fullerene anion into a semiconductor nanoparticles SnO_2.

Fullerenes, namely C_{60} and C_{70}, as well as water soluble derivatives of C_{60} bearing charged functional groups form optically transparent microscopic clusters (aggregates) in mixed solvents at room temperature.[14–17] Clustering of fullerene molecules is mainly associated with the strong three-dimensional hydrophobic interactions between fullerene units. Details on the conditions for forming fullerene clusters,[14, 16, 18, 19] size distribution studies,[16] and their spectroscopic properties[16, 20] have already been reported. Clusters of C_{70} have also been shown to facilitate charge transport across a bilayer membrane.[21] We have recently reported a remarkable property of stabilizing photogenerated charge transfer

---

[a] Dr. P. V. Kamat, S. Barazzouk, Dr. K. G. Thomas
Notre Dame Radiation Laboratory, Notre Dame
Indiana 46556-0579 (USA)
E-mail: pkamat@nd.edu, georgetk@md3.vsnl.net.in

[b] S. Barazzouk, Dr. S. Hotchandani
Groupe de Recherche en Énergie et Information Biomoléculaires
Université du Québec à Trois Rivières
Québec, G9A 5H7 (Canada)
E-mail: hotchand@uqtr.uquebec.ca

[c] Dr. K. G. Thomas
Photochemistry Research Unit
Regional Research Laboratory, Trivandrum (India)

0947-6539/00/0621-3914 $ 17.50+.50/0

products in the clusters of C_{60}–aniline dyads.[19] Relatively long-lived C_{60} anion in these systems (lifetimes $\sim 100\,\mu s$) was attributed to the electron-hopping phenomenon within the clusters of such dyads. A major challenge for mimicking photosynthesis is the efficient utilization of such custom-synthesized systems of the acceptor–bridge–donor type.

Several researchers have employed different methods to cast photoactive fullerene films, but with a limited success.[22–24] Ordered surfaces of C_{60} have also been formed on pyrolytic graphite (HOPG) by vapor deposition.[25] A major problem in these studies is the inability to cast relatively thick fullerene films for absorbing the incident light efficiently. These films absorb less than 1 % of incident light and generate photocurrents less than $1\,\mu A\,cm^{-2}$. In contrast, organic dye sensitized photoelectrochemical cells deliver significantly higher power conversion efficiencies (2–5 %).[26–28] Such a competitive edge demands new methodologies to improve the light harvesting efficiency of fullerene-based compounds in photoelectrochemical cells. The first step in this direction would be to increase the surface area by introducing a nanostructured morphology for the photoactive films. Such an approach of developing nanostructured metal oxide film has been proved to be useful in the design of dye sensitized photoelectrochemical cells.[29, 30] By making use of a similar concept we recently adopted an electrodeposition technique to cast relatively thick C_{60} films from a cluster (aggregate) solution of acetonitrile/toluene 3:1 mixture.[31] The nanostructured C_{60} cluster films cast on SnO_2 films were photoelectrochemically active with a two to three orders of enhancement in the photocurrent generation.

We have now carried out a detailed investigation of the electrodeposition of fullerene–aniline dyad clusters, that is $(C_{60}\text{–aniline})_m$, on nanostructured SnO_2 films (Scheme 2). The nanostructured SnO_2 film cast on an optically transparent electrode not only serves as a template for electrodeposition, but also, acts as an efficient electron collector from the C_{60}-radical anion. Overall, it is possible to achieve two to three orders of magnitude enhancement in the surface area by using nanostructured SnO_2 template. The results that elucidate the photoinduced charge transfer in these cluster films cast on nanostructured SnO_2 substrates and their photoelectrochemical properties are described here.

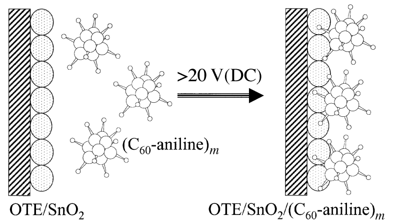

Scheme 2. Electrodeposition of $(C_{60}\text{–aniline})_m$ dyad clusters on nanostructured SnO_2 films.

Experimental Section

Material and methods: The synthesis of *para*-substituted fullerene–aniline dyad and pyrrolidinofullerene (Scheme 3) has been described elsewhere.[4, 19] These compounds are readily soluble in nonpolar solvents such as toluene. In mixed solvents, however, they aggregate and form larger clusters. Nanostructured SnO_2 films were cast on an optically transparent electrode (OTE) by applying a dilute (1–2 %) colloidal solution (Alfa Chemicals) and annealing the dried film at 673 K. Details on the electrode preparation and its properties are described elsewhere.[32] These films are highly porous and are electrochemically active to conduct charges across the film.

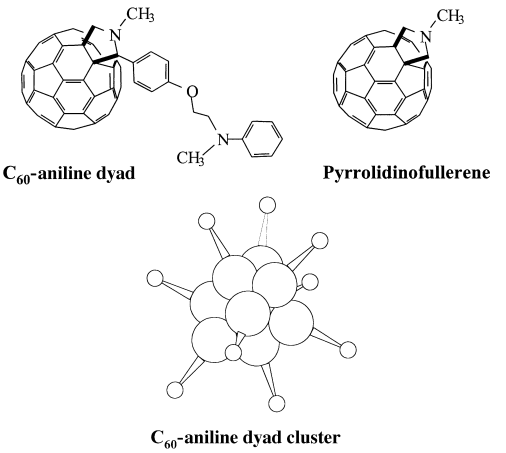

Scheme 3. Fullerene monomers and clusters.

The SnO_2-film electrode (OTE/SnO_2) and a OTE plate were introduced in a 1 cm path length cuvette and were connected to positive and negative terminals of the power supply, respectively. A known amount (~ 2 mL) of a C_{60}–aniline dyad cluster (0.11 mM) solution in acetonitrile/toluene 3:1 was transferred to a cuvette in which the two electrodes (namely OTE/SnO_2 and OTE) were kept at a distance of ~ 6 mm with Teflon spacer. A DC voltage (5–200 V) was applied between these two electrodes with a Fluke 415 power supply (Figure 1). The deposition of the film can be visualized as the solution turns colorless with simultaneous brown coloration of the SnO_2/OTE electrode. (The dyad cluster coated electrode will be referred with the notation, $OTE/SnO_2/(C_{60}\text{–aniline})_m$.)

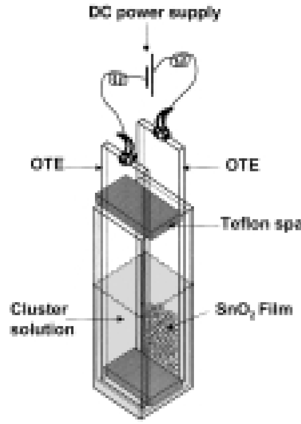

Figure 1. Representation of the electrodeposition setup used in the preparation of the dyad films electrodes.

Spectroelectrochemical experiments were performed by transferring the cell assembly into the sample compartment of the spectrophotometer. The electrodes were kept parallel to the probe beam. This configuration allowed us to monitor the changes in the absorbance of cluster suspension during the application of a DC voltage applied potential. The UV/Vis spectra were recorded on a Shimadzu 3101 or a Cary 50 spectrophotometer. The emission spectra of the cluster films (C_{60}–aniline dyad and the model compound, pyrrolidinofullerene) were recorded using a SLM S1000 spectrofluorimeter in the front-face configuration. Dynamic light scattering studies were carried out using a Coulter model N4 plus particle size analyzer. Transmission electron micrographs (TEM) of C_{60} clusters were recorded by applying a drop of the sample to carbon-coated copper grid. Images were recorded at a magnification of 150000 times using an Hitachi H600 transmission electron microscope.

Laser flash photolysis: Nanosecond laser flash photolysis experiments were performed with a nitrogen laser system (337 nm, 6 ns pulse width, 2–4 mJ per pulse). The OTE/SnO_2/(C_{60}–aniline)$_m$ was kept in a rectangular cuvette that had provision for flowing the nitrogen gas. A typical experiment consisted of a series of 2–3 replicate shots per single measurement. The average signal was processed with a Le Croy digitizer. Details of the experimental set up can be found elsewhere.[33]

Photoelectrochemical measurements: These measurements were carried out with a standard three-compartment cell consisting of a working electrode and Pt wire gauze counter electrode. All photoelectrochemical measurements were carried out in 0.5 M LiI and 1 mM I_2 in acetonitrile. Photocurrent measurements were made with a Keithley model 617 programmable electrometer. A collimated light beam from a 150 W Xenon lamp with a 425 nm cut-off filter was used for excitation of the C_{60}–aniline films cast on SnO_2 electrodes. A Bausch and Lomb high intensity grating monochromator was introduced into the path of the excitation beam for selecting wavelength. A Princeton Applied Research (PAR) model 173 potentiostat and Model 175 universal programmer were used for recording I/V characteristics.

Results and Discussion

Growth of C_{60}–aniline clusters in solution: The C_{60}–aniline dyad is soluble in nonpolar solvents such as toluene, but readily forms aggregate clusters in a mixture of polar and nonpolar solvents. For example, the cluster suspension of C_{60}–aniline dyad can be prepared by injecting toluene solution of the C_{60}–aniline dyad into acetonitrile (acetonitrile/toluene 3:1 *v*/*v*). The absorption spectra of C_{60}–aniline dyad formed in neat toluene and acetonitrile/toluene 3:1 are compared in Figure 2. The dyad clusters exhibit a structureless broad absorption in the 400–750 nm region and exhibit higher molar extinction coefficients than the parent C_{60}–aniline dyad. These optically transparent clusters are stable at room temperature and can be reverted back to the monomeric forms by diluting with toluene.

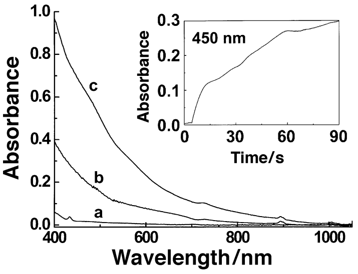

Figure 2. Absorption spectra of C_{60}–aniline dyad (0.11 mM) in a) toluene and b) toluene/acetonitrile 1:3 *v*/*v*. Spectrum c) was recorded after the cluster suspension was subjected to a DC electric field (5 V) for 90 s. The insert shows the absorption growth at 450 nm during the application of an applied DC electric field (5 V).

Upon subjecting the cluster suspension to a low electric (DC) field (< 5 V) we observe an increase in the absorption throughout the visible region (spectrum c in Figure 2). By maintaining the electrode parallel to the probe beam we were able to monitor the changes in the absorption spectrum of the cluster suspension during the application of DC voltage. The spectrum of the inset in Figure 2 shows the increase in absorbance of the cluster suspension at 450 nm for a period of 1.5 min. This increase in molar absorbancy is indicative of a growth in cluster size of the fullerene–aniline dyads. Such a growth in cluster size arises from the charging of clusters during the application of electric field, which is succeeded by the association of smaller clusters to form larger ones (Reaction (1)). To the best of our knowledge this is the first such observation to grow fullerene clusters under the influence of a DC electric field.

$$(C_{60}\text{–aniline})_m + (C_{60}\text{–aniline})_n \xrightarrow{<5\text{ V DC}} (C_{60}\text{–aniline})_{m+n} \qquad (1)$$

Upon examining the cluster suspension with particle size analyzer and transmission electron microscopy, we observe an increased average particle diameter from 160 nm to ~200 nm (Figure 3). The particle size distribution as measured from dynamic light scattering measurements is shown in Figure 3A.

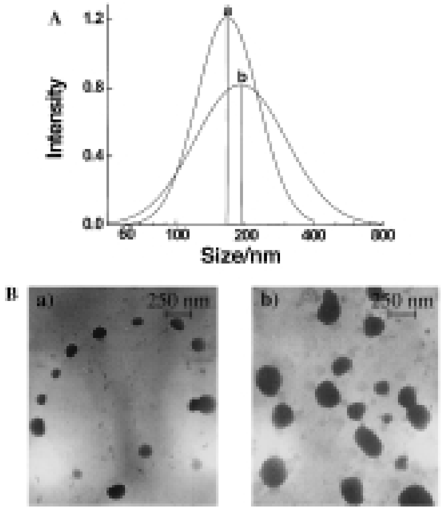

Figure 3. A) Particle size distribution of C_{60}–aniline dyad clusters with dynamic light scattering method: a) Before and b) after subjecting the cluster suspension to a DC electric field (5 V) for 90 s. B) Transmission electron micrographs of the samples in A).

The electron micrographs of the dyad clusters before and after subjecting the suspension in acetonitrile/toluene 3:1 to 5 V DC electric field are shown in Figure 3B. The growth of average particle diameter from 160 nm to 200 nm following the application of a DC electric field represents an increase in the average volume of clusters by a factor of two. There were no noticeable electrochemical changes occurring during these experiments since the DC current was too small.

Electrodeposition of C_{60}–aniline clusters as thin films: At greater DC voltages (> 20 V) we observed a different behavior of these clusters. Within a few seconds of DC voltage application, the cluster suspension in the spectroelectrochemical cell turned colorless and all C_{60}–aniline dyad clusters got deposited as a brown film on the positive electrode. Figure 4A shows the absorption spectrum of nanostructured SnO_2 film cast on an optically transparent elec-

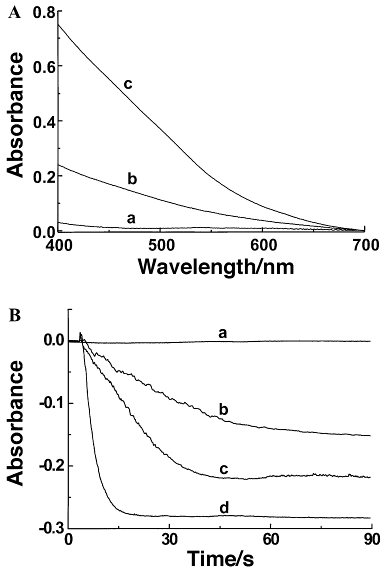

Figure 4. A) The absorption spectra of a) OTE/SnO_2, b) OTE/SnO_2/(C_{60} – aniline)$_m$, and c) OTE/(C_{60} – aniline)$_m$. B) The disappearance of C_{60} – aniline dyad clusters in 1:3 toluene/acetonitrile during the application of electric field. The absorbance at 450 nm was monitored at different applied potentials: a) 0 V, b) 50 V, c) 100 V, and d) 200 V. In situ absorbance measurements were carried out by keeping the cell assembly in the sample compartment of the spectrophotometer. The cell configuration was such that the probe beam was parallel to the two electrodes.

trode before and after the deposition of the C_{60} – aniline dyad clusters. The absorption features of electrodeposited cluster film are quite broad and are similar to the ones observed in solution (Figure 2). Such a broad spectral feature has also been noted in pristine C_{60} films which seem to arise from intermolecular interaction between fullerene moieties.[34] The broad absorption of these films in the visible and in the near IR region makes these films an ideal candidate for solar energy conversion applications.

The deposition rate was followed by monitoring the absorbance of C_{60} – aniline dyad cluster in the solution during our spectroelectrochemical experiment. As the C_{60} clusters were deposited onto the electrode surface, the absorbance of the solution decreased. The absorption of the cluster solution at 450 nm monitored during the application of DC voltage is shown in Figure 4B. Within a matter of few seconds entire C_{60} – aniline dyad clusters disappeared from the solution; this indicates a faster deposition rate for these cluster films. The deposition rate was dependent on the applied DC voltage and increased from 0.03 s^{-1} to 0.3 s^{-1} when the applied potential was increased from 50 to 200 V. Although we do not expect any major electrolysis to occur during our low current experiments, some charging of these clusters is evident. The fact that the deposition occurs only at the positive electrode indicates that the fullerene clusters carry a net negative charge during the period of electrodeposition. We can therefore conclude that the applied electric field is responsible for charging up the medium that surrounds the clusters with a net negative charge followed by their deposition as thin film on the electrode surface. If the applied DC field is not strong enough to carry out deposition, the electrostatic effects between the clusters dominate and further lead to aggregation. The observed increase in the cluster size (Figure 3) supports the aggreagtion of fullerene clusters at low DC applied voltages.

The thickness of the C_{60} – aniline dyad cluster film can be varied either by changing the concentration of the C_{60} – aniline dyad clusters or varying the time of deposition. The electrodeposited film was thoroughly washed with acetonitrile following the electrodeposition experiment. Unless otherwise specified the amount of C_{60} – aniline dyad deposited on the film was 0.2 $\mu mol\,cm^{-2}$ (approx. 1.44 μm in thickness). The C_{60} – aniline dyad cluster films were physically and chemically stable and did not deteriorate during the electrochemical and photoelectrochemical measurements.

The films deposited on nanostructured SnO_2 films were uniform and robust compared with those deposited directly on conducting glass plates. The SnO_2 films (1 – 2 μm thickness) cast on OTE electrodes are highly porous and serve as a template for the electrodeposition of C_{60} – aniline dyad clusters. We will refer these electrodes as OTE/SnO_2/(C_{60} – aniline)$_m$ in our future discussions. It should be noted that preformed clusters in solution is an essential requirement to electrodeposit fullerene films on electrode surfaces. Attempts to electrodeposit films directly from neat toluene solution containing C_{60} or C_{60} – aniline dyad solution were not successful.

Emission properties: The emission from excited singlet fullerenes, monofunctionalzed pyrrolidine derivatives (reference compound) and fullerene – aniline dyads (Scheme 2) are useful for probing the excited state deactivation processes. At room temperature the fullerene clusters exhibit a weak emission band in the red region (700 – 800 nm) corresponding to 0 – 0 transition ($S_1 \rightarrow S_0$). As shown in our previous studies the clusters of pyrrolidinofullerene exhibit an emission maximum at 740 nm in nonpolar solvents.[19] A significant decrease in the fluorescence yield was observed for fullerene – aniline dyad clusters.

In the present study we compared the emission intensity of fullerene – aniline dyad cluster films with that of a pyrrolidinofullerene cluster films deposited on OTE/SnO_2 electrodes. While the singlet excited state of reference compound pyrrolidino fullerene cluster is deactivated through radiative and intersystem crossing pathways, an additional deactivation pathway, namely intramolecular electron transfer, dominates in the case of fullerene – aniline dyads (Reactions 2 – 5).

$$\mathrm{OTE/SnO_2/(C_{60}-aniline)}_m + h\nu \rightarrow \mathrm{OTE/SnO_2/(C_{60}-aniline)}_m{}^*(\mathrm{S_1}) \qquad (2)$$

$$\mathrm{OTE/SnO_2/(C_{60}-aniline)}_m{}^*(\mathrm{S_1}) \rightarrow \mathrm{OTE/SnO_2/(C_{60}-aniline)}_m + h\nu' \qquad (3)$$

$$\mathrm{OTE/SnO_2/(C_{60}-aniline)}_m{}^*(\mathrm{S_1}) \xrightarrow{\mathrm{ISC}} \mathrm{OTE/SnO_2/(C_{60}-aniline)}_m{}^*(\mathrm{T_1}) \qquad (4)$$

$$\mathrm{OTE/SnO_2/(C_{60}-aniline)}_m{}^*(\mathrm{S_1}) \xrightarrow{\mathrm{ET}} \mathrm{OTE/SnO_2/(C_{60}{}^{-}\text{-}aniline^{+})}_m \qquad (5)$$

ISC and ET refer to intersystem crossing and electron transfer, respectively. (It should be noted that intracluster interactions between the donor and acceptor species of different dyad molecules could also induce charge transfer since these dyad molecules are deposited as closely packed clusters.)

0947-6539/00/0621-3917 $ 17.50+.50/0

Figures 5A and B show the emission spectra of electrodeposited cluster films of pyrrolidinofullerene and fullerene–aniline dyad, respectively in air and in acetonitrile. In the absence of any solvent both the cluster films are fluorescent and exhibit emission maximum at 740 nm. However, when the cluster films were brought in contact with a polar solvent, acetonitrile, we observed a decrease in fluorescence yield. While this decrease in fluorescence intensity is small (~30%) for pyrrolidinofullerene cluster films, the decrease in the fluorescence yield of C_{60}–aniline dyad film in acetonitrile was significant (>90%). Almost all the fluorescence was quenched as the C_{60}–aniline dyad cluster film came in contact with the polar solvent. (The small decrease in fluorescence of pyrrolidinofullerene film in acetonitrile is likely to arise from the changes in the refractive index of the medium, solvent polarity effects and/or alteration in the collection intensity of the emitting light.)

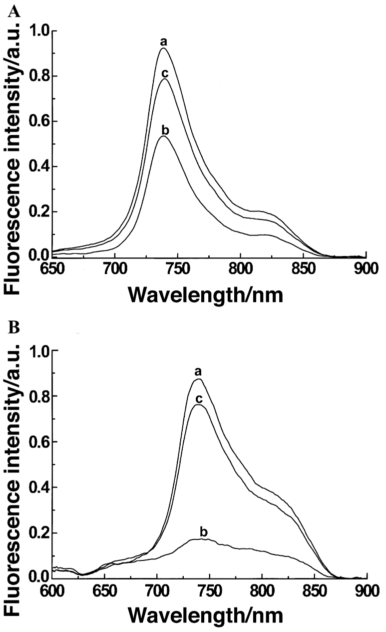

Figure 5. Emission spectra of the cluster film cast on OTE/SnO_2 electrode using front face excitation geometry (excitation at $\lambda = 470$ nm). A) The reference compound, (pyrrolidinofullerene) and B) C_{60}–aniline dyad cluster films: a) in air, b) after contact with acetonitrile, and c) same film dried by purging with nitrogen gas.

In order to ascertain the role of acetonitrile in facilitating the deactivation of the $(C_{60}\text{–aniline})_m$ singlet excited state through intramolecular charge transfer we dried both these films in the sample chamber of the spectrofluorimeter by flushing with nitrogen gas. As the solvent was evaporated off with the flow of nitrogen gas we were able to restore most (nearly 90%) of the original emission (spectrum c in Figure 5). Thus, it is evident that the polar solvent surrounding the C_{60}–aniline dyad clusters plays an important role in inducing intramolecular charge separation and charge stabilization. Similar observations on the solvent polarity effect on the fluorescence quenching intramolecular charge separation and charge stabilization of C_{60}–donor dyads have been made earlier with fullerene–aniline dyad molecules in various solvents.[4, 35] The generation of charge separated radical pair was observed only in the polar solvents. On the other hand population of triplet excited state was observed in nonpolar solvents. The fluorescence quenching results of Figure 5 confirm that the charge separation sensitivity of the C_{60}–aniline dyad molecules are retained even when they are deposited as cluster films.

Intramolecular charge transfer in fullerene–aniline dyad clusters: If indeed the fluorescence quenching observed in Figure 5B is the result of photoinduced charge transfer in C_{60}–aniline dyad cluster film (Reaction 5), we should be able to probe the formation of C_{60} anion in a nanosecond laser flash photolysis set up. A thin film of C_{60}–aniline dyad clusters deposited on a transparent OTE/SnO_2 electrode was inserted in a closed sample cell that had provision to purge with nitrogen. The electrode was immersed in a pool of deaerated acetonitrile solution and was excited with a 337 nm laser pulse. The transient absorption spectra recorded 10 μs following 337 nm laser pulse excitation (Figure 6A) shows the characteristic C_{60}-anion band with a maximum at 1020 nm. The absorption time profile (Figure 6B) recorded at a monitoring wavelength of 1020 nm shows the contribution of two species. The fast decay component which corresponds to the deactivation of the triplet excited state, is followed by a long-lived absorption that extends up to ~200 μs. This long-lived absorption corresponds to C_{60}-anion radical as confirmed from the transient spectrum recorded after the disappearance of triplet excited state.

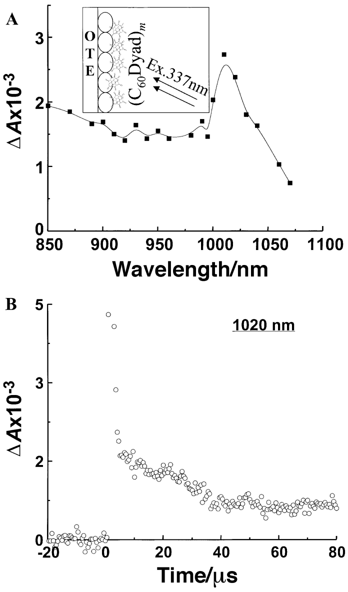

Figure 6. A) Transient absorption spectrum recorded 10 μs after 337 nm laser pulse excitation of OTE/SnO_2/$(C_{60}\text{–aniline})_m$ electrode. The electrode was immersed in a deaerated acetonitrile solution. B) Absorption-time profile at 1020 nm recorded after 337 nm excitation of OTE/SnO_2/$(C_{60}\text{–aniline})_m$ electrode was immersed in a deaerated acetonitrile solution.

Our earlier cluster studies in acetonitrile/toluene medium have elucidated the influence of solvent polarity and the role of clusters in photoinduced charge separation and charge

0947-6539/00/0621-3918 $ 17.50+.50/0

stabilization.[19] In the present study we have demonstrated the feasibility of achieving intramolecular (as well as intracluster) charge transfer in thin films of the fullerene – aniline dyad clusters. Noteworthy, however, is that the absorption band at 1020 nm survives for a long time and can be seen even at a time interval of $>100\,\mu$s after laser pulse excitation. The formation of such a long-lived charge separated pair in a dyad system is very important in designing light energy conversion systems. To the best of our knowledge this is the first spectroscopic demonstration of achieving long-lived charge separation in a fullerene based donor – acceptor thin films.

Fullerene – aniline dyad films as photosensitive electrodes: There have been few attempts earlier to cast donor – bridge – acceptor molecules as thin films on electrode surfaces and employ them as photosensitive electrodes.[23, 36–38] Often such systems produce low photocurrent as charge recombination process competes with the charge collection at the electrode surface. Since cluster formation is a useful approach for circumventing the back electron transfer process in the donor – bridge – acceptor systems, it should be possible to utilize fullerene – aniline dyad cluster films for harnessing light energy quite efficiently.

We employed OTE/SnO_2/(C_{60} – aniline)$_m$ as a photoanode in a photoelectrochemical cell. Figure 7A shows the photocurrent generation following the excitation of C_{60} – aniline cluster films with visible light ($\lambda > 425$ nm). The photocurrent generation was prompt and responded to on/off cycles of illumination. The stability of photocurrent was dependent on the type of redox couple employed. Under visible light irradiation ($\lambda > 425$ nm) and with I_3^-/I^- as a redox couple, the photoelectrochemical cell delivered a stable photocurrent of ~ 0.2 mA cm^{-2} and an open circuit voltage of ~ 170 mV. The I^-/I_3^- redox couple employed in the photoelectrochemical cell ensured quick regeneration of the fullerene – aniline dyad clusters in the film. The power characteristics of this photoelectrochemical cell (Figure 7B) shows a drop in photovoltage and increase in the photocurrent as we decrease the load resistance. The cell exhibits a fill factor of 0.32 and a net power conversion efficiency of ~ 0.01 % under high intensity irradiations (110 mW cm^{-2}). At low intensity excitation (1 mW cm^{-2}) we observed a ten-fold higher power conversion efficiency of 0.1 %.

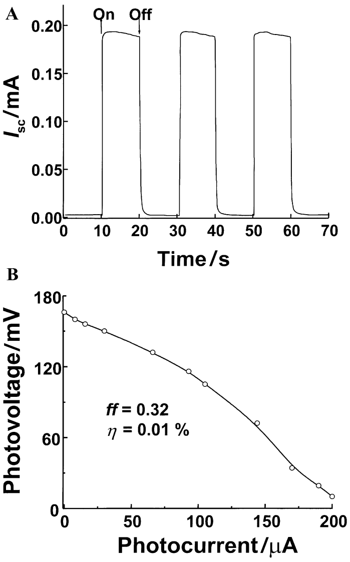

Figure 7. A) Generation of photocurrent at OTE/SnO_2/(C_{60} – aniline)$_m$ electrode under visible light ($\lambda > 425$ nm) excitation. Blank OTE/SnO_2 electrodes under the same irradiation conditions yield negligible photocurrents (Electrolyte: 0.5 M LiI, 1 mM I_2 in acetonitrile). B) Power characteristics of the photoelectrochemical cell employing OTE/SnO_2/(C_{60} – aniline)$_m$ electrode (Electrolyte: 0.5 M LiI, 1 mM I_2 in acetonitrile, $\lambda >$ 425 nm).

The photocurrents observed in the present study are two to three orders of magnitude greater than the recently reported photoelectrochemical cells using functionalized fullerenes[22, 24] and an order of magnitude greater than the photovoltaic cell designed with a C_{60} – oligophenylenevinylene.[39] Note that the photocurrent measurements in the present study were done with a yellow corning filter (425 nm cutoff), which only allow for long wavelength excitations.

Under visible light illumination, the OTE/SnO_2/(C_{60} – aniline)$_m$ electrode shows remarkable rectification behavior in the potential range of -360 to 240 mV vs Ag/AgCl. The electron flow towards the collecting electrode can be controlled by the application of an electrochemical bias. Figure 8 shows the I/V characteristics of OTE/SnO_2/(C_{60} – aniline)$_m$ electrode in dark and under visible light irradiation. At negative potentials (< -300 mV) we see a decrease in the photocurrent as electrons accumulate within the SnO_2 nanocrystallites, thus, suppressing the charge transport to the collecting OTE surface. Since the electrode is susceptible to direct reduction of C_{60} – aniline dyad clusters at negative potentials, the scan was initiated at -300 mV. As the applied potential was scanned towards the positive potentials, we observed an increase in the photocurrent generation. The photocurrent became steady at potentials greater than -200 mV. Increased charge separation and the facile transport of charge carriers under positive bias resulted in enhanced photocurrent generation. At potentials greater than 0.35 mV vs Ag/AgCl, the electrochemical oxidation of iodide interferred with the photocurrent measurements. (The increase in the dark current can be seen in Figure 8.)

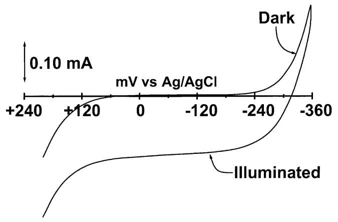

Figure 8. I/V characteristics of OTE/SnO_2/(C_{60} – aniline)$_m$ electrode in dark and under visible light irradiation ($\lambda > 425$ nm). (CE: Pt and RE: Ag/AgCl. Electrolyte: 0.5 M LiI, 1 mM I_2 in acetonitrile).

The photocurrent action spectrum of C_{60} film cast on a nanostructured SnO_2 electrode is shown in Figure 9. The IPCE values were calculated by normalizing the photocurrent values for incident light energy and intensity.[32] A broad response in the visible with photoconversion efficiencies

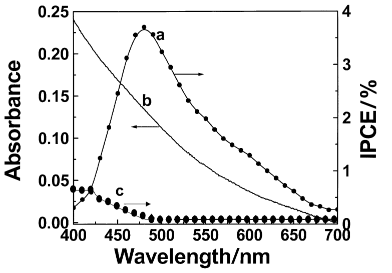

Figure 9. a) Photocurrent action spectrum and b) absorption spectrum of OTE/SnO_2/(C_{60} – aniline)$_m$ electrode. c) Photocurrent action spectrum of blank OTE/SnO_2 electrode is shown for comparison. (CE: Pt; Electrolyte: 0.5 M LiI, 1 mM I_2 in acetonitrile).

decreasing with increasing wavelengths is observed for OTE/SnO_2/(C_{60} – aniline)$_m$ electrode. The overall response parallels the broad spectral features observed in the absorption spectra, thus confirming the excitation of C_{60} film as the origin of photocurrent generation. Interestingly, however, these electrodes show significant photoresponse in the red region. A maximum IPCE of ~4% was observed in the wavelength region of 450 nm. Inner filter effects resulted in decreased IPCE at wavelengths below 450 nm. Also, at wavelengths below 400 nm, direct excitation of SnO_2 film would dominate the photocurrent generation.

The photocurrent generation in these films is initiated by the photo-induced charge separation in dyad clusters (Reaction 5). As shown in Figure 6, the C_{60} anion in these fullerene cluster films survives for a long time ($>200\,\mu s$). The charge separated pair in fullerene – aniline dyad cluster is stabilized as the electrons hop away to the neighboring fullerene moieties. A similar mechanism also occurs in the C_{60} – aniline dyad cluster films deposited on OTE/SnO_2. Both the photoinduced charge transfer within the C_{60} – aniline dyad cluster and the electron transfer from reduced fullerene moiety ($E(C_{60}/C_{60}^{-}) \approx -0.2$ V vs NHE) into SnO_2 nanocrystallites (E_{CB} (SnO_2) = 0.0 V vs NHE) are thermodynamically favored processes (Figure 10). While the reduced anion moeity of the dyad cluster injects electrons into the SnO_2 nanocrystallites, the oxidized aniline counterpart undergoes charge transfer with the iodide in the electrolyte (Reactions 6 and 7).

$$(C_{60}^{-} - \text{aniline}^{+})_m + SnO_2 \rightarrow (C_{60} - \text{aniline}^{+})_m + SnO_2(e^{-}) \quad (6)$$

$$2(C_{60} - \text{aniline}^{+})_m + 3\,I^{-} \rightarrow 2\,(C_{60} - \text{aniline}) + I_3^{-} \quad (7)$$

The electrons transferred to the semiconductor nanocrystallites are collected at the OTE surface and are driven to the counter electrode through an external circuit to regenerate the redox couple. It should be noted that when C_{60} – aniline dyad films were cast on a nanostructured TiO_2 film, we observed negligibly small photocurrents. Since the conduction band of TiO_2 ($E_{CB} = -0.5$ V vs NHE) is more negative than the reduction potential of fullerene (C_{60}), the reduced form of the fullerene – aniline dyad is unable to transfer the electrons to TiO_2 (Figure 10).

Previous attempts[22, 24] to employ C_{60} and functionalized fullerenes as electrode materials have failed to generate photocurrents ($<1\,\mu A\,cm^{-2}$) that are comparable to other organic dye based photoelectrochemical cells.[26, 27, 40] These researchers have employed relatively thin fullerene films, which exhibit poor light harvesting and charge separation efficiencies. We are able to overcome these limitations by using an electrodeposition approach of casting nanostructured fullerene – aniline dyad cluster films. The beneficial aspects of increased absorption of the incident light, long-lived charge separated pair, efficient charge transport within the film and quick regeneration of the sensitizer achieved in the present study demonstrate a new promise of using functionalized fullerenes in light harvesting applications.

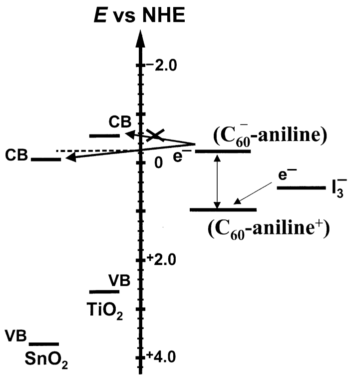

Figure 10. Energy level diagram illustrating the mechanism of charge transfer in a OTE/SnO_2/(C_{60} – aniline)$_m$ system.

Conclusion

A new methodology has been developed for growing fullerene aggregate clusters under the influence of a DC electric field. Controlled growth of these clusters in acetonitrile/toluene mixture can be achieved by controlling the applied voltage. At potentials greater than 20 V, charged clusters get deposited as thin films on the positive electrode surface. The electrodeposited fullerene cluster films are electrochemically and photoelectrochemically active. They are capable of delivering relatively large photocurrents when employed as photoanodes in photoelectrochemical cells. The improved performance of these fullerene electrodes is attributed to the increased molar absorptivity in the visible region, long-lived charge separation, and production of electroactive C_{60}-anion moieties that are capable of delivering charges to SnO_2 nanocrystallites. The potential dependent phenomenon of casting thin films on electrode surfaces has opened up new avenues to utilize fullerene – bridge – donor type dyad molecules in energy conversion devices.

Acknowledgements

The research described herein was supported by the Office of Basic Energy Science of the Department of the Energy. We would like to thank Dr. V. Biju of RRL, Trivandrum for the providing the fullerene samples. S.B. and S.H. acknowledge the support of Natural Sciences and Engineering Research Council of Canada. This is contribution NDRL 4219 from the Notre Dame Radiation Laboratory.

[1] D. Kuciauskas, S. Lin, G. R. Seely, A. L. Moore, T. A. Moore, D. Gust, T. Drovetskaya, C. A. Reed, P. D. W. Boyd, *J. Phys. Chem.* **1996**, *100*, 15926.

[2] N. Martin, B. Sanchez, B. Illescas, I. Perez, *Chem. Rev.* **1998**, *98*, 2527.

[3] F. Diederich, M. Gómez-López, *Chem. Soc. Rev.* **1999**, 263.

[4] K. George Thomas, V. Biju, M. V. George, D. M. Guldi, P. V. Kamat, *J. Phys. Chem. B* **1999**, *103*, 10755.

[5] D. M. Guldi, *Chem. Commun.* **2000**, 321.

[6] P. V. Kamat, K. D. Asmus, *Interface* **1996**, *5*, 22–25.

[7] G. Yu, J. Gao, J. C. Hummelen, F. Wudl, A. J. Heeger, *Science* **1995**, *270*, 1789.

[8] V. I. Srdanov, C. H. Lee, N. S. Sariciftci, *Thin Solid Films* **1995**, *257*, 233.

[9] L. Smilowitz, N. S. Sariciftci, R. Wu, C. Gettinger, A. J. Heeger, F. Wudl, *Phys. Rev. B Condens. Matter* **1993**, *47*, 13835.

[10] B. Miller, J. M. Rosamilia, G. Dabbagh, R. Tycko, R. C. Haddon, A. J. Muller, W. Wilson, D. W. Murphy, A. F. Hebard, *J. Am. Chem. Soc.* **1991**, *113*, 6291.

[11] Y. Wang, *Adv. Photochem.* **1995**, *19*, 179.

[12] S. Licht, O. Khaselev, P. A. Ramakrishnan, D. Faiman, E. A. Katz, A. Shames, S. Goren, *Solar Energy Mater. Solar Cells* **1998**, *51*, 9.

[13] G. Yu, Gao J, J. C. Hummelen, F. Wudl, A. J. Heeger, *Science* **1995**, *270*, 1789.

[14] Y. M. Wang, P. V. Kamat, L. K. Patterson, *J. Phys. Chem.* **1993**, *97*, 8793.

[15] M. Sundahl, T. Andersson, K. Nilsson, O. Wennerstrom, G. Westman, *Synth. Met.* **1993**, *55*, 3252.

[16] Y.-P. Sun, B. Ma, C. E. Bunker, B. Liu, *J. Am. Chem. Soc.* **1995**, *117*, 12705.

[17] A. Beeby, J. Eastoe, R. K. Heenan, *J. Chem. Soc. Chem. Commun.* **1994**, 173.

[18] S. Nath, H. Pal, D. K. Palit, A. V. Sapre, J. P. Mittal, *J. Phys. Chem. B* **1998**, *102*, 10158.

[19] K. George Thomas, V. Biju, M. V. George, D. M. Guldi, P. V. Kamat, *J. Phys. Chem. B* **1999**, *103*, 8864.

[20] D. M. Guldi, H. Hungerbuehler, K. D. Asmus, *J. Phys. Chem.* **1995**, *99*, 13487.

[21] S. F. Niu, D. Mauzerall, *J. Am. Chem. Soc.* **1996**, *118*, 5791.

[22] W. Zhang, Y. Shi, L. Gan, C. Huang, H. Luo, D. Wu, N. Li, *J. Phys. Chem. B* **1999**, *103*, 675.

[23] T. Akiyama, H. Imahori, A. Ajawakom, Y. Sakata, *Chem. Lett.* **1996**, 907.

[24] H. Imahori, T. Azuma, A. Ajavakom, H. Norieda, H. Yamada, Y. Sakata, *J. Phys. Chem. B* **1999**, *103*, 7233.

[25] P. Janda, T. Krieg, L. Dunsch, *Adv. Mater.* **1998**, *10*, 1434.

[26] S. Ferrere, A. Zaban, B. A. Gregg, *J. Phys. Chem. B* **1997**, *101*, 4490.

[27] K. Sayama, M. Sugino, H. Sugihara, Y. Abe, H. Arakawa, *Chem. Lett.* **1998**, 753.

[28] A. C. Khazraji, S. Hotchandani, S. Das, P. V. Kamat, *J. Phys. Chem. B* **1999**, *103*, 4693.

[29] M. Graetzel in *Semiconductor Nanoclusters—Physical, Chemical and Catalytic Aspects* (Eds.: P. V. Kamat, D. Meisel), Elsevier Science, Amsterdam, **1997**, p. 353.

[30] P. V. Kamat in *Nanoparticles and Nanostructural Films* (Ed.: J. H. Fendler), Wiley-VCH, New York, **1998**, p. 207.

[31] P. V. Kamat, S. Barazzouk, K. George Thomas, S. Hotchandani, *J. Phys. Chem. B* **2000**, *104*, 4814.

[32] I. Bedja, S. Hotchandani, P. V. Kamat, *J. Phys. Chem.* **1994**, *98*, 4133.

[33] M. D. Thomas, G. L. Hug, *Comput. Chem.* **1998**, *22*, 491.

[34] U. Jonas, F. Cardullo, P. Belik, F. Diederich, A. Gugel, E. Harth, A. Herrmann, L. Isaacs, K. Müllen, H. Ringsdorf, C. Thilgen, P. Uhlmann, A. Vasella, C. W. M. Waldraff, *Chem. Eur. J.* **1995**, *1*, 243.

[35] R. M. Williams, J. M. Zwier, J. W. Verhoeven, *J. Am. Chem. Soc.* **1995**, *117*, 4093.

[36] R. Argazzi, C. A. Bignozzi, T. A. Heimer, F. N. Castellano, G. J. Meyer, *J. Am. Chem. Soc.* **1995**, *117*, 11815.

[37] H. Imahori, Y. Sakata, *Eur. J. Org. Chem.* **1999**, 2445.

[38] S. Cattarin, P. Ceroni, D. M. Guldi, M. Maggini, E. Menna, F. Paolucci, S. Roffia, G. Scorrano, *J. Mater. Chem.* **1999**, *9*, 2743.

[39] J.-F. Nierengarten, J.-F. Eckert, J.-F. Nicoud, L. Ouali, V. Krasnikov, G. Hadziioannou, *J. Chem. Soc. Chem. Commun.* **1999**, 617.

[40] I. Bedja, P. V. Kamat, S. Hotchandani, *J. Appl. Phys.* **1996**, *80*, 4637.

Received: April 10, 2000 [F2411]

0947-6539/00/0621-3921 $ 17.50+.50/0